Petroleum Science 20 (2023) 2531–2544

Contents lists available at ScienceDirect

Petroleum Science

journal homepage: www.keaipublishing.com/en/journals/petroleum-science

Original Paper

Magnetic core-shell microparticles for oil removing with thermal driving regeneration property

Shi-Hao Chen, Chuan-Lin Mou*, Wen-Long Ma, Ya-Dong Li, Zi-Yu Tang, Hong-Bo Deng**

College of Chemistry and Chemical Engineering, Southwest Petroleum University, Chengdu, Sichuan, 610500, China

ARTICLE INFO

Article history:
Received 25 June 2022
Received in revised form
14 November 2022
Accepted 14 February 2023
Available online 16 February 2023

Edited by Jia-Jia Fei

Keywords:
Microfluidics
Core-shell microparticles
Thermal driving regeneration
Secondary pollution
Oil adsorption

ABSTRACT

Here, we report the construction of magnetic core-shell microparticles for oil removal with thermal driving regeneration property. Water-in-oil-in water (W/O/W) emulsions from microfluidics are used as templates to prepare core-shell microparticles with magnetic holed poly (ethoxylated trimethylolpropane triacrylate) (PETPTA) shells each containing a thermal-sensitive poly (*N*-Isopropylacrylamide) (PNIPAM) core. The microparticles could adsorb oil from water due to the special structure and be collected with a magnetic field. Then, the oil-filled microparticles would be regenerated by thermal stimulus, in which the inner PNIPAM microgels work as thermal-sensitive pistons to force out the adsorbed oil. At the same time, the adsorbed oil would be recycled by distillation. Furthermore, the adsorption capacity of the microparticles for oil keeps very stable after 1st cycle. The adsorption and regeneration performances of the microparticles are greatly affected by the size of the holes on the outer PETPTA shells, which could be precisely controlled by regulating the interfacial forces in W/O/W emulsion templates. The optimized core-shell microparticles show excellent oil adsorption and thermal driving regeneration performances nearly without secondary pollution, and would be a reliable green adsorption material for kinds of oil.

1. Introduction

Growing water pollution has had a significant negative influence on the environment and people, and it has sparked considerable concern in nations all over the world (Qiu, 2010; Wang and Yang, 2016). Oily wastewater discharged recklessly into rivers, lakes, and oceans would degrade water quality and raise the possibility of sickness, death, and the extinction of species (Yu et al., 2017; Adetunji and Olaniran, 2021; de Medeiros et al., 2022). Petroleum exploitation continuously creates large amounts of wastewater containing crude oil, tar, and petroleum products, and they could cause serious water pollution without adequate treatment (Whitehead and Dubansky, 2012; Beyer et al., 2016; Soares and Teixeira, 2020). There are three main categories of oil removal methods: physical, chemical, and biological, such as booms (Shi et al., 2017), skimmers (Broje and Keller, 2007), *in-situ* combustion (Rojas-Alva et al., 2019), chemical dispersion (Zeinstra-Helfrich et al., 2017), and biodegradation of oil (Omarova and Swientoniewski, 2019), which are mainly used for the preliminary treatment of oily wastewater. At present, the deep treatment of oily wastewater can be divided into flocculation (Ma et al., 2021), membrane filtration (El-Samak et al., 2020), flotation (Li et al., 2015), and adsorption. Flocculation method is high-cost due to the production of sludge and non-recyclable flocculants. Membrane filtration method has some disadvantages such as complex procedure and poor tolerance. Flotation method has high equipment costs and maintenance costs. Due to its low cost, environmental friendliness, straightforward technique and design, high performance, great chemical and thermal durability, and high capacity, the adsorption method is the most extensively utilized technology among them. However, the poor regenerative property is a serious drawback of the adsorption method (Pan et al., 2016; Yu et al., 2020).

Recently, a variety of innovative adsorption materials, including membrane materials, modified textiles, metal-organic frameworks (MOFs), aerogels, and sponges/foams have been developed. These materials come in various forms and are addressed with numerous

* Corresponding author.
** Corresponding author.
E-mail addresses: mouchl@163.com (C.-L. Mou), denghongbo@swpu.edu.cn (H.-B. Deng).

https://doi.org/10.1016/j.petsci.2023.02.010

different recycling methods. For example, for solvent cleaning method, the oil adsorbed on the fibrous membrane and nanofiber/nanonet membrane can be efficiently cleaned by organic solvents (El-Samak et al., 2020; Doan and Vo, 2021), to achieve the recycling of the membranes. The adsorption performance of the membranes remains unchanged with multiple uses. However, the organic solvents tend to cause secondary pollution. For pH-responsive method, the adsorption/desorption of magnetic textile with pH-responsive can be controlled by adjusting pH value of solutions, resulting in regeneration of adsorbents (Yan et al., 2019). However, utilizing substances that are acidic or alkaline can cause secondary pollution. The photocatalytic method involves the generation of photoelectric behavior of photo-responsive TiO_2 in MS@TiO_2@PPy (Melamine Sponge-co-TiO_2-co-Poly-pyrrole) monoliths or ZnO in cotton textiles with visible light, which decomposes the adsorbed oil to regenerate the adsorbents (Chen et al., 2015; Yang et al., 2019; Yan and Li, 2020). In that way, this method can effectively avoid secondary pollution and reduce the cost of wastewater treatment, however, the adsorbed oil cannot be recycled for reuse. For distillation/vacuum drying method, the regeneration of AM-rGAs (Amylamine-modified MOF-co- reduced graphene oxide aerogel) with saturated adsorption of various oil molecules is accomplished by vacuum drying at the boiling temperature of the absorbed oil substance (Sun et al., 2020). The aerogel could maintain stable adsorption performance even after 50 cycles, however, the adsorbate oil cannot be recycled. Extrusion is a method for regenerating polyurethane sponge/foam and aerogel with porous structures and good elastic properties (Lin et al., 2019; Lv et al., 2019; Wu et al., 2019; Le et al., 2020). The materials can be regenerated without secondary pollution, and valuable oil can also be reused, however, the adsorption performance of such adsorbents decreases significantly. Therefore, a regeneration method for achieving adsorption/desorption of adsorbents by adjusting the temperature is proposed. In addition, the above adsorbents can only achieve high yields in large-scale scenarios. Microparticles with smaller size and larger specific surface area are suitable for more scenes (Gu et al., 2014; Pan et al., 2016; Tao et al., 2017), but the regeneration methods of microparticles are the same as that of the above adsorbents, like solvent cleaning (Abbaspourrad et al., 2013; Dutra et al., 2017; Lu et al., 2017; Shao et al., 2019; Theurer et al., 2020; Yu et al., 2020), pH-responsive (Wu and Honciuc, 2018), photocatalytic (Chen et al., 2015), distillation (Tao et al., 2017; Liu et al., 2019), vacuum drying (Gu et al., 2014; Mi et al., 2020), ultrasonic washing (Mao et al., 2014; Peng et al., 2018), and thermos-sensitive (Lu et al., 2020), which would cause similar problems. Consequently, research has focused on development of microparticles with thermal driving regeneration property to avoid secondary pollution as well as adsorption and recovery of oil.

Here, we report the construction of microparticles with magnetic holed shells each containing a thermal-sensitive core for oil removal with thermal driving regeneration property (Fig. 1). Monodispersed water-in-oil-in-water (W/O/W) emulsions, containing *N*-Isopropylacrylamide (NIPAM) in the aqueous cores and ethoxylated trimethylolpropane triacrylate (ETPTA), magnetic Fe_3O_4 nanoparticles in the middle oil layer, are prepared in a two-staged capillary microfluidic device (Fig. 1a). The W/O/W emulsions could be controlled evolved to different structures by adjusting the interfacial tension in the emulsions (Fig. 1b1, b2 and b4). After UV induced polymerization, the evolved emulsions will convert to microparticles with magnetic holed poly (ethoxylated trimethylolpropane triacrylate) (PETPTA) shells each containing a thermal-sensitive poly (*N*-Isopropylacrylamide) (PNIPAM) core with varied structures (Fig. 1b3 and b5). When the ambient temperature is higher than the volume phase transition temperature (VPTT) of PNIPAM, the inner cores will shrink and the oil around microparticles will be adsorbed into the holed shells due to the special structure (Fig. 1c1 and c2). Then, the microparticles with adsorbed oil could be transferred to water with a magnet (Fig. 1c3). When the ambient temperature is lower than the VPTT of PNIPAM, the thermal-sensitive core will swell to force out adsorbed oil from the microparticle like a piston and the core-shell microparticle is regenerated. (Fig. 1c4). At the same time, the released oil could be recycled. In the regeneration process of the core-shell microparticles, no organic solvents are involved. The adsorption and regeneration performances of the core-shell microparticles are optimized by regulating the structure of the evolved emulsions. In the cyclic adsorption/regeneration process, the oil removal ability of the core-shell microparticles is also stable. This research offers a novel way to construct environmentally friendly oil absorbent.

2. Experimental section

2.1. Materials

N-Isopropylacrylamide (NIPAM) was purchased from Tokyo Chemical Industry Co., Ltd. (Tokyo, Japan), which was purified and recrystallized by dissolving it in n-hexane/acetone mixture (50/50, V/V). *N*, *N*'-methylenebis(acrylamide) (MBA) and 2,2'-azobis(2-methylpropionamidine) dihydrochloride (V-50) were purchased from Shanghai Aladdin Biochemical Technology Co., Ltd (Shanghai, China), and used as a cross-linker and a water-soluble UV initiator respectively. Pluronic F-127 (F-127) as a water-soluble surfactant was obtained from Sigma-Aldrich (Saint Louis, Missouri, America). Ethoxylated trimethylolpropane triacrylate (ETPTA) and glycerol were purchased from Shanghai Aladdin Biochemical Technology Co., Ltd. (Shanghai, China). 2-hydroxy-2-methylpropiophenone (HMPP) was obtained from Shanghai Aladdin Biochemical Technology Co., Ltd. (Shanghai, China) as an oil-soluble UV initiator. Benzyl benzoate (BB) was purchased from Sinopharm Chemical Reagent Co., Ltd. (Shanghai, China). Hydroxyethyl cellulose (HEC) was purchased from Kelon Chemical (Chengdu, China). Iron(II) chloride tetrahydrate and ferric chloride hexahydrate were purchased from Shanghai Maclean's Biochemical Technology Co., Ltd (Shanghai, China) and Damao Chemical Reagent Factory (Tianjin, China) respectively, and were used to synthesize Fe_3O_4 nanoparticles and oil-based magnetic fluids according to the literature (Yu et al., 2020). Other solvents and chemicals are analytical grades.

2.2. Microfluidic device

Based on the previously reported method (Wang and Zhang, 2013), the microfluidic device was a coaxial microchannel structure composed of two square capillary tubes and three cylindrical glass capillary tubes (Fig. 1a). Here, the inner diameters of the injection tube, transition tube, and collection tube were 550 μm, 220 μm, and 400 μm respectively, and the outer diameters of the capillary tubes were 960 μm. The injection tube and transition tube were tailored by a micropuller (PN-30, Narishige, Tokyo, Japan) and a microforge (MF-830, Narishige, Tokyo, Japan); the outer diameter of the outlet of the transition tube was approximately 80 μm and the inner diameter of the outlet of injection tube was approximately 120 μm. And the inner diameters of the square capillary tubes were 1 mm, which matched the outer diameter of the cylindrical glass capillary to form a good coaxial geometry. Finally, the tubes were connected and sealed with epoxy resin.

2.3. Preparation of monodispersed W/O/W emulsions

Monodispersed W/O/W emulsions were produced within a microfluidic device and served as templates for preparing core-

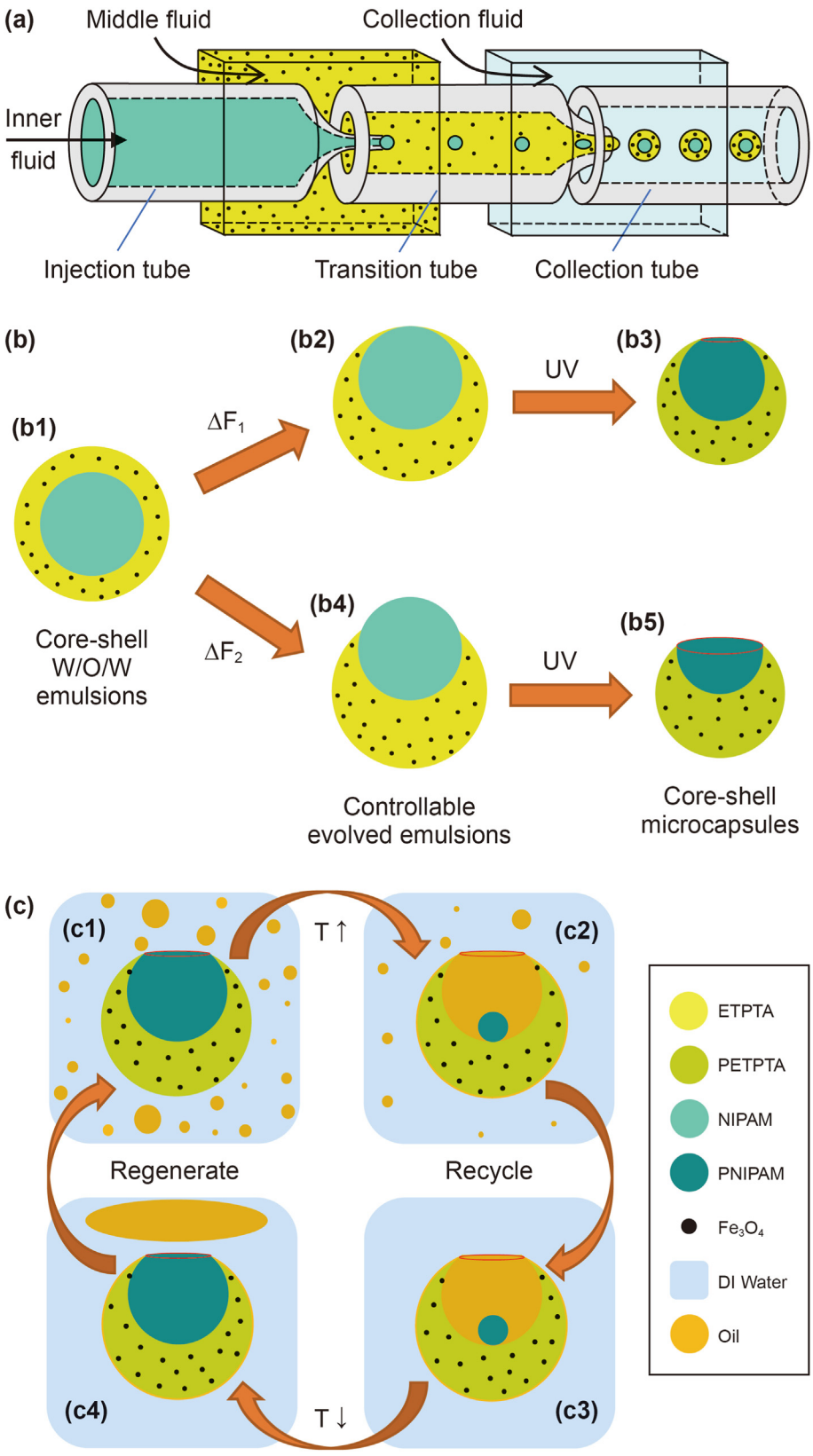

Fig. 1. Schematic illustration of the preparation procedure and the function of core-shell microparticles. (**a**) NIPAM contained inner aqueous fluid is infused into the injection tube, at the same time, ETPTA and magnetic Fe_3O_4 particles contained middle fluid is introduced into the transition tube, to prepare monodisperse water-in-oil-in-water (W/O/W) emulsions in a two-stage microfluidic device. (**b**) The W/O/W emulsions will evolve to different structure by the controlled adhesion energy (ΔF) (**b1**, **b2**, **b4**). The evolved W/O/W emulsions are polymerized by UV irritation and will convert to core-shell microparticles each with a single-holed PETPTA shell and a thermal-sensitive PNIPAM core (**b3**, **b5**). (**c**) Recyclable oil adsorption of core-shell microparticles. The inner PNIPAM cores could shrink by rising the ambient temperature and the oil will adsorbed into the PETPTA shells (**c1**, **c2**). The oil-contained core-shell microparticles could be collected by magnet and regenerated by temperature-controlled release the captured oil (**c3**, **c4**).

shell microparticles each possessing a single hole. In the microfluidic device, three injection pumps were utilized to inject the inner aqueous fluid, the middle oil fluid and the outer aqueous fluid into the injection tube, the transition tube and the collection tube respectively. The inner aqueous fluid was composed of DI water (5 mL), NIPAM (1.13 g), MBA (0.031 g), V-50 (0.05 g) and F-127 (0.05 g); the middle oil fluid was a mixture of ETPTA (8 mL) and BB (2 mL, 20% v/v), containing HMPP (0.1 mL) and magnetic Fe_3O_4 nanoparticles (0.01 g); the outer aqueous fluid was DI water (100 mL) containing F-127 (0.5 g), HEC (0.5 g) and glycerol (5.0 g). The HEC is added to increase the viscosity of the aqueous fluid. The middle oil fluid is easier to shear off with aqueous fluid of higher viscosity in microfluidic operation process. Moreover, the stability of the emulsions is affected by the viscosity and density difference of each fluid, which is critically important for the successful conversion of emulsions to microparticles (Mou and He, 2012). Glycerol (1.26 g/mL) could increase viscosity and density of the aqueous fluid, which is beneficial to enhance the stability of the resulting emulsions. The flow rates of the inner aqueous fluid, middle oil fluid, and outer aqueous fluid were 30 μL/min, 35 μL/min, and 400 μL/min respectively. W/O emulsions were formed by emulsifying the NIPAM-contained aqueous fluid as the inner phase and the oil fluid containing ETPTA at the conical end of the injection tube; the W/O emulsions and the aqueous fluid containing glycerol were further emulsified at the conical end of the transition tube to produce monodispersed W/O/W emulsion templates (Fig. 1b1). Subsequently, the generated W/O/W emulsions were collected in a container containing collection solution.

2.4. Preparation of core-shell microparticles

Core-shell microparticles each with a controllable single-hole shell were fabricated by adjusting the ratio of ETPTA and BB in the middle oil phase of emulsions under ultraviolet (UV) irradiation. We demonstrate the fabrication of core-shell microparticles that the collected emulsions were placed under UV light for 5 min to initiate the polymerizations of the internal aqueous phase containing NIPAM and photoinitiator V-50 and the oil phase containing ETPTA and photoinitiator HMPP. Then, the monodispersed W/O/W emulsions convert to core-shell microparticles each with a magnetic single-holed PETPTA shell and a thermo-sensitive PNIPAM core. Due to the volume contraction triggered by the rapid polymerization of the oil phase, and the interaction force of the inner and middle phases, the single-holes are formed (Guzowski et al., 2012; Wang and Zhang, 2013). The microparticles were washed with DI water and ethanol to remove residual components.

2.5. Monodispersity of W/O/W emulsions and core-shell microparticles

The morphologies of the W/O/W emulsions and the core-shell microparticles were observed using a CCD camera installed on an optical microscope (IX31, Olympus, Japan). The diameters of the inner and outer phases of the W/O/W emulsions and the core-shell microparticles were measured by commercial size-analysis software (JIFEI, Nanjing Yifei Science and Technology Ltd., Nanjing, China). The size distribution of emulsions and microparticles was analyzed with Microsoft office excel. The coefficient of variation (*CV*) is defined as the ratio of the standard deviation to the average diameter and is used to estimate the size monodispersity of the samples. More than 100 droplets/microparticles were counted to guarantee statistical representation. The *CV* value was obtained by the following formula:

$$CV = 100\% \times \left(\sum_{i=1}^{N} (D_i - \overline{D_n})^2 \Big/ \Big(N - 1\Big) \right)^{\frac{1}{2}} \Big/ \overline{D_n} \quad (1)$$

where D_i is the diameter of microspheres, N is the total number of microspheres counted, $\overline{D_n}$ is the arithmetic mean diameter. According to this formula, when the *CV* value is less than 5%, the emulsions/microparticles should be monodispersed.

2.6. Influence of benzyl benzoate (BB) volume fraction of oil phase on W/O/W emulsions and core-shell microparticles

In the W/O/W emulsions, a stable equilibrium three-phase system consists of an inner aqueous phase containing NIPAM, a middle oil phase containing ETPTA, and an outer aqueous phase, where the inner and middle layers are in contact with each other but immiscible, both immersed in the outer aqueous solution (Guzowski et al., 2012). In equilibrium, controllable configurations of W/O/W emulsions from complete-engulfing to partial-engulfing are regulated by the interfacial tensions between the three-phase solutions, which is associated with an equation (Wang and Zhang, 2013): $\Delta F = \gamma_{IM}+\gamma_{MO}-\gamma_{Film}$, where γ_{IM} represents the interfacial tension between the inner and middle phases, and γ_{MO} represents the interfacial tension between the middle and outer phases, and γ_{Film} is the tension of the thin film between inner and outer phases. For calculation of ΔF, γ_{IM} and γ_{MO} are measured by the pendent-drop method using an integrated measurement system of interface parameters (KRUSS DSA30S, Germany); γ_{Film} is obtained from adhesion experiments of inner-fluid and outer-fluid drops in middle oil solution according to force balance (Poulin and Bibette, 1998). Furthermore, precise manipulation of pore size of the core-shell microparticles is achieved by inducing evolution of W/O/W emulsions through adjustment of BB volume fraction. The measurement method of pore sizes is the same as Section 2.5.

2.7. Magnetic characterization of core-shell microparticles

Recent developments in microsized adsorbents have incorporated magnetism, offering convenience and allowing easy recovery of adsorbents (Lu et al., 2020; Mi et al., 2020; Yu et al., 2020). Magnetic Fe_3O_4 nanoparticles of the middle oil phase were responsible for the recyclability of core-shell microparticles. Core-shell microparticles with magnetic oil shells were generated from stable W/O/W emulsions. Therefore, the stability of the ETPTA oil solution precursor fluid containing magnetic particles and oil-based magnetic fluid, respectively, were investigated. According to Section 2.3, two ETPTA oil solutions were prepared with the same composition, and the magnetic particles and the oil-based magnetic fluid were added separately to the oil solutions. Subsequently, these solutions were dispersed homogeneously and their stabilities were obtained with a digital camera after 12 h. The hysteresis curves of Fe_3O_4 nanoparticles and core-shell microparticles with magnetic oil shells were measured by Vibrating Sample Magnetometer (VSM). The recyclability of core-shell microparticles was investigated by a simple method that core-shell microparticles were moved according to a route with a magnet.

2.8. The contact angles between ETPTA oil plates and water/diesel oil

The adsorption capacity of core-shell microparticles is influenced by the lipophilicity of ETPTA oil shells that is directly reflected by the contact angle between ETPTA oil shells and water/diesel. ETPTA oil solutions with BB volume fractions of 0%, 10%, 20%,

30%, and 40% were placed in a mold and polymerized under UV stimulation to generate ETPTA oil plates. With an integrated measurement system of interface parameters (KRUSS DSA30S, Germany), the contact angles between ETPTA oil plates and water/diesel oil were measured after cleaning the oil plates with DI water and ethanol.

2.9. Temperature-dependent equilibrium volume change of PNIPAM microgels in core-shell microparticles

Adsorption/regeneration capacity of core-shell microparticles was achieved by thermo-sensitive of PNIPAM microgels in core-shell microparticles. PNIPAM microgel has been widely applied due to its excellent thermal driving property, whose volume phase transition temperature (VPTT) in water is 32 °C (Sun and Qing, 2011; Mou and Ju, 2014; Mou and Wang, 2018). The microparticles were put in a special glass slide container on a microscope-mounted heating and cooling stage, and the volume changes of microparticles were recorded with an optical microscope and an automatic analysis program. The ambient temperature of the microparticles was set in the range of 23 °C to 40 °C. Microparticles at the predetermined temperatures have been kept for more than 30 min before each measurement to enable their equilibrium phase state to be reached. The volume change rate of PNIPAM microgels can be calculated as follows:

$$S = 100\% \times \left(\sum_{i=1}^{N} V_{i1} / V_{i0} \right) \Big/ N \tag{2}$$

V_{i0} is the volume of the initial hydrogel when it swells. V_{i1} is the volume of the final hydrogel when contracted. N is the number of test samples.

2.10. Adsorption and regeneration test

2.10.1. Microscopic characterization of oil adsorption/regeneration process of core-shell microparticles

Adsorption/regeneration process of core-shell microparticles was recorded with an optical microscope and an automatic analysis program. Diesel oil dyed by Sudan III was placed on a special slide containing DI water, and the microparticles were randomly sprinkled on the liquid surface. Then, the ambient temperature of the microparticles was set in the range of 23 °C to 40 °C by a thermostatic stage system. Especially, during the regeneration of the diesel oil, the microparticles needed to be shaken to allow the shrinking hydrogels in the cores to come into contact with water and swell by adsorbing water.

2.10.2. Macroscopic characterization of oil adsorption/regeneration process of core-shell microparticles

Adsorption/regeneration process of core-shell microparticles was recorded with a digital camera. In the following three ways, there was a significant adsorption effect of microparticles on diesel oil. (1) The microparticles were randomly sprinkled on the liquid surface of floating diesel oil dyed by Sudan III, and the ambient temperature was controlled with a thermostat water bath. After complete adsorption, the microparticles were collected with a magnet. (2) The microparticles were placed in a glass bottle with homogeneous dispersion of DI water and diesel oil, and the ambient temperature was controlled with a thermostat water bath. After complete adsorption, the microparticles were transferred to another bottle with a magnet. Then, diesel oil was regenerated by the microparticles in a cooling-up and shaking process. (3) The microparticles were attracted to one side of a transparent pipe with a magnet. The ambient temperature was changed by using a homogeneous mixture of DI water and diesel oil heated in advance.

2.10.3. Quantitative analysis of oil adsorption/regeneration process of core-shell microparticles

The recyclability of core-shell microparticles was achieved due to the thermo-sensitive core and magnetic shell of the microparticles. Then, the adsorption capacity of the microparticles was quantified in the above way (1). The total weight of the glass bottle, deionized water, and oil was recorded as M_1; and the weight of the microparticles was recorded as M_2. After an adsorption process, the microparticles containing diesel oil were transferred by a magnet, and the total weight of the glass bottle, deionized water, and oil was recorded as M_3. The weights were measured with an analytical balance. The oil adsorption capacity is obtained according to the following formula:

$$H = (M_1 - M_3) / M_2 \tag{3}$$

According to the above way, the adsorption/regeneration process is repeated 10 times and the oil adsorption capacity of each time is recorded. Meanwhile, the adsorption capacity of soybean oil and ethylene glycol dimethacrylate (EGDMA) by microparticles is studied with the same method.

3. Results and discussion

3.1. Morphology and structure of monodispersed W/O/W emulsions and core-shell microparticles

Fig. 2 demonstrates microscope photographs and size distributions of monodispersed W/O/W emulsions and core-shell microparticles. The W/O/W emulsions were fabricated from a microfluidic device, and were uniform in structure, as shown in Fig. 2a. And Fig. 2b shows that the size distribution of W/O/W emulsions, the average diameters of the W/O/W emulsions and the inner aqueous droplets were 252.2 μm and 174.6 μm respectively (*CV* of D_e and D_i are 2.76% and 2.02% respectively). The monodispersed W/O/W emulsions were gathered in the collection solution and subsequently subjected to UV light in an ice water bath. Water-soluble photo initiator V-50 and oil-soluble photo initiator HMPP induced the cross-linking polymerizations of NIPAM-contained aqueous phase and ETPTA-contained oil phase, respectively, under UV irradiation (Wang and Zhang, 2013). After 5 min, the W/O/W emulsions were converted to core-shell microparticles with single-hole shells and hydrogel cores (Fig. 2c). The average diameters of core-shell microparticles and the inner cores were 236.0 μm and 165.8 μm respectively (*CV* of D_s and D_c are 2.96% and 1.75% respectively) (Fig. 2d). According to the *CV* and the size distributions, the W/O/W emulsions and the core-shell microparticles were monodispersed. The result demonstrates that the size of microparticles could be precisely controlled by adjusting the generation of monodispersed W/O/W emulsions.

3.2. Influence of benzyl benzoate (BB) volume fraction of oil phase on W/O/W emulsions and core-shell microparticles

The main purpose for adding benzyl benzoate into the middle oil phase is regulation to the interfacial tension of the oil phase and the neighboring aqueous phases, which will influence the structure of the achieved microparticles (Guzowski et al., 2012; Wang and Zhang, 2013). From Table S1, with the increase of BB volume content, the interfacial tension between the inner phase and the middle phase changes from 2.95 mN/m to 4.56 mN/m, and the interfacial tension between the middle phase and the outer phase

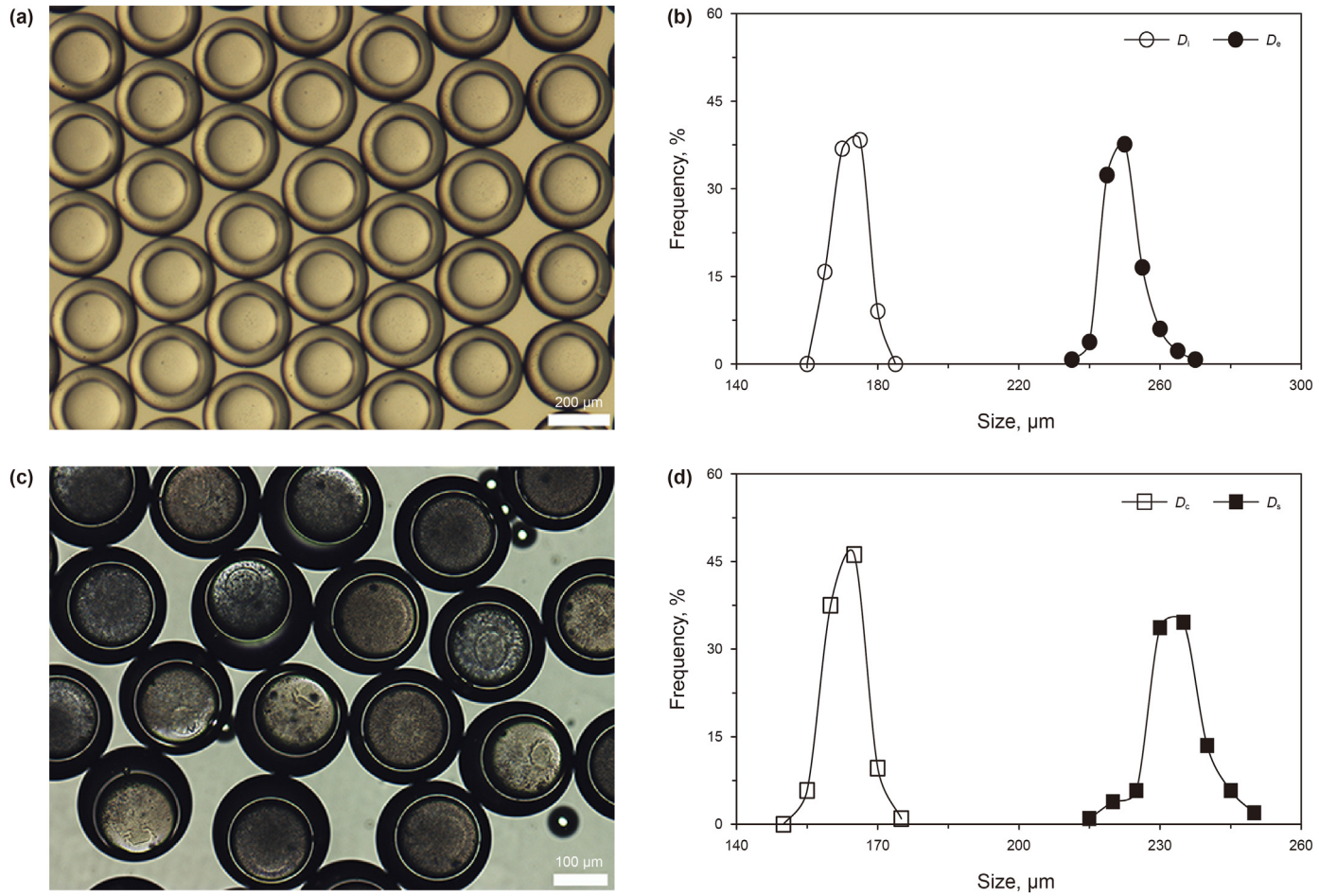

Fig. 2. Preparation of W/O/W emulsions and core-shell microparticles. (**a**) Optical micrograph and (**b**) the corresponding size distribution of W/O/W emulsions. D_e and D_i are the diameters of W/O/W emulsions and the inner aqueous droplets. (**c**) Optical micrograph of core-shell microparticles and (**d**) the corresponding size distribution of the diameter of the PETPTA shells and inner PNIPAM cores in DI water at room temperature. D_s and D_c represent the outer diameter of the PETPTA shell and inner PNIPAM microgels. Scale bars are 200 μm in (**a**) and 100 μm in (**c**).

changes from 5.35 mN/m to 7.53 mN/m, and the interfacial tension of the film changes from 8.3 mN/m to 10.87 mN/m. According to the equation: $\theta_{IM} = \arccos\left(\left(\gamma_{Film}^2 - \gamma_{IM}^2 - \gamma_{MO}^2\right)/2\gamma_{IM}\gamma_{MO}\right)$, the contact angle θ_{IM} between the inner drop and the middle oil phase reaches from 0° to 53.7°, which means the W/O/W emulsions controllable evolve from complete-engulfing to partial-engulfing configuration and the structure of the achieved microparticles changes from core-shell spheroidal to bowl-shaped (Fig. 3a, b and g). Moreover, the pore size of the achieved microparticles increases from 54 μm to 98 μm with the increase of the BB volume fraction (Fig. 3c–e and h), and the pore size distribution frequency of the microparticles is shown in Fig. S1. Therefore, the structure of the core-shell microparticles could be precisely controlled by manipulating the BB volume fraction of the middle oil phase in the emulsions.

3.3. Magnetic property of microparticles

The magnetism facilitates the collection of microparticles, and the stability of the emulsions containing Fe_3O_4 is of great importance in the controllable achievement of the core-shell microparticles. The ETPTA oil phase containing magnetic nanoparticles was stratified after 12 h (Fig. S2), while the ETPTA oil phase containing oil-based magnetic fluid remained evenly dispersed. Therefore, the magnetism of the nanoparticles was achieved by oil-based magnetic fluid, which could maintain the stability of emulsions. Besides, Fig. 4 shows that hysteresis curves of the Fe_3O_4 magnetic nanoparticles (Fig. 4a) and core-shell microparticles respectively (Fig. 4b), and their saturation magnetic moments are 1.5983 emu and 0.1355×10^{-2} emu respectively (saturation magnetizations are 65.50 emu/g and 11.22×10^{-2} emu/g respectively). Therefore, the microparticles could be controlled with a magnetic field (Yu et al., 2020). And there was no obvious remanence or coercivity, confirming the microparticles are superparamagnetic (Lu et al., 2020; Mi et al., 2020). Furthermore, the microparticles could be precisely moved according to a route by a magnet (Fig. 4c). Hence, the microparticles exhibit a reliable magnetic collection property.

3.4. Wettability of PETPTA oil plates

The wettability of PETPTA oil shell of the microparticles is a crucial factor for the adsorption of the core-shell microparticles. The contact angles between ETPTA oil plates generated from ETPTA oil solutions with BB volume fractions of 0%, 10%, 20%, 30%, and 40% respectively and water were 59.59°, 62.31°, 64.01°, 56.08°, and 60.65° respectively (Fig. 5a). And the contact angles between ETPTA oil plates generated from ETPTA oil solutions with BB volume fractions of 0%, 10%, 20%, 30%, and 40% respectively and water were

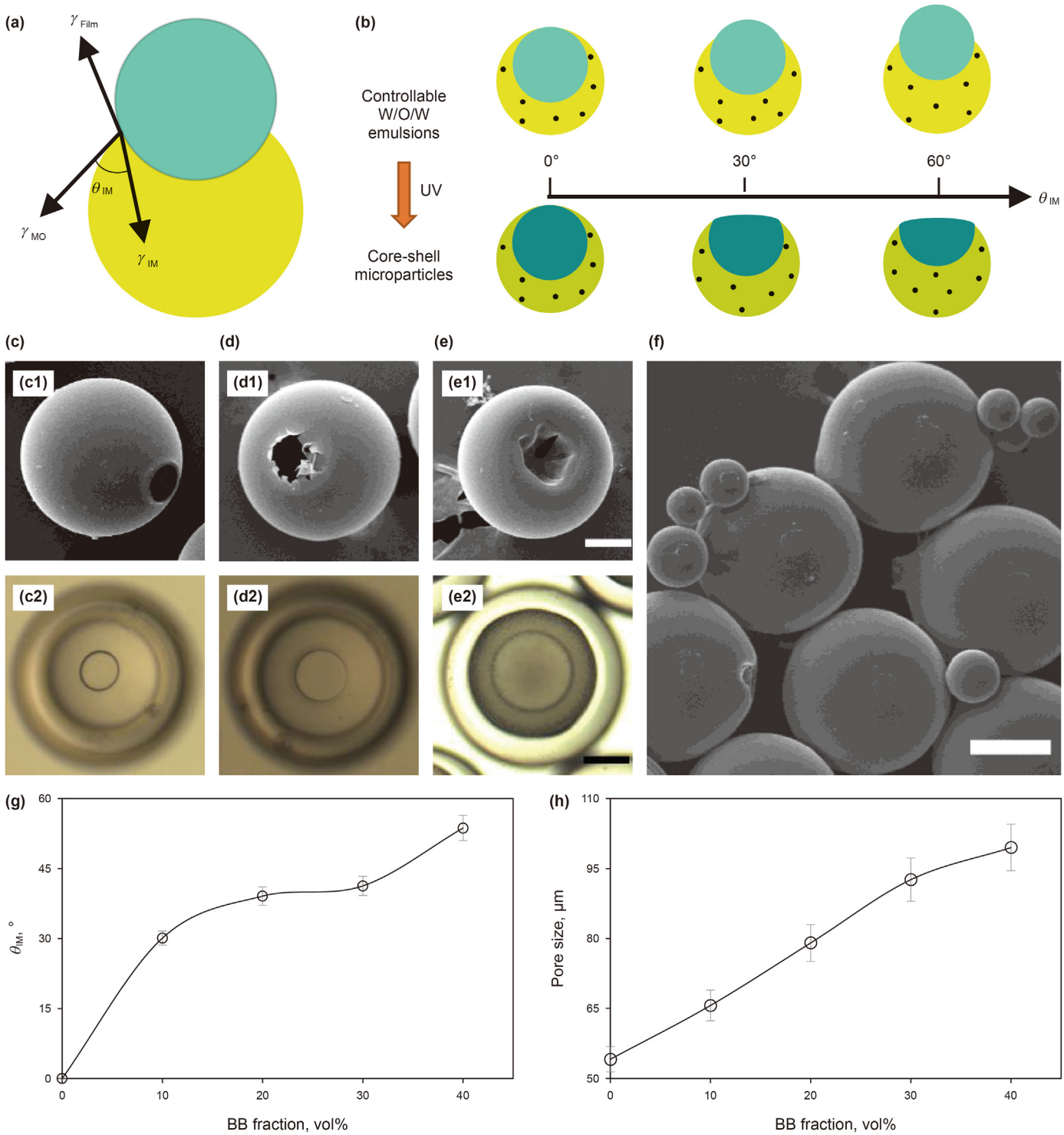

Fig. 3. Core-shell microparticles with varied holes size on the shells. (**a**) Force analysis of controlled evolution process of W/O/W emulsion. (**b**) Influence of θ_{IM} on the structure of W/O/W emulsions and the holes size on the resulting shells. The contact angle θ_{IM} between inner phase and outer phase can be calculated by γ_{IM}、γ_{MO} and γ_{Film}. (**c**–**e**) SEM, (**c1**–**e1**) images and optical micrograph, (**c2**–**e2**) of core-shell microparticles with varied holes size on the shells. Scale bars are 50 μm. (**f**) SEM image of hole-shells and escaped cores. Scale bar is 100 μm. (**g**) Inflence of benzyl benzoate content on the θ_{IM} of W/O/W emulsions. (**h**) The average pore size on the shells.

26.51°, 19.46°, 24.30°, 21.74°, and 20.02° respectively (Fig. 5b), confirming the PETPTA oil plate is hydrophilic and highly oleophilic. At the same time, the added benzyl benzoate will not involve in the polymerization reaction, which will not affect the property of the resulting PETPTA shells. In the adsorption process, the oil of wastewater can be adsorbed on the microparticles due to the highly lipophilic shell. In the regeneration process, the regeneration property of the microparticles could be assisted by a hydrophilic PETPTA shell due to the PNIPAM core needing to adsorb water to swell to force out adsorbed oil.

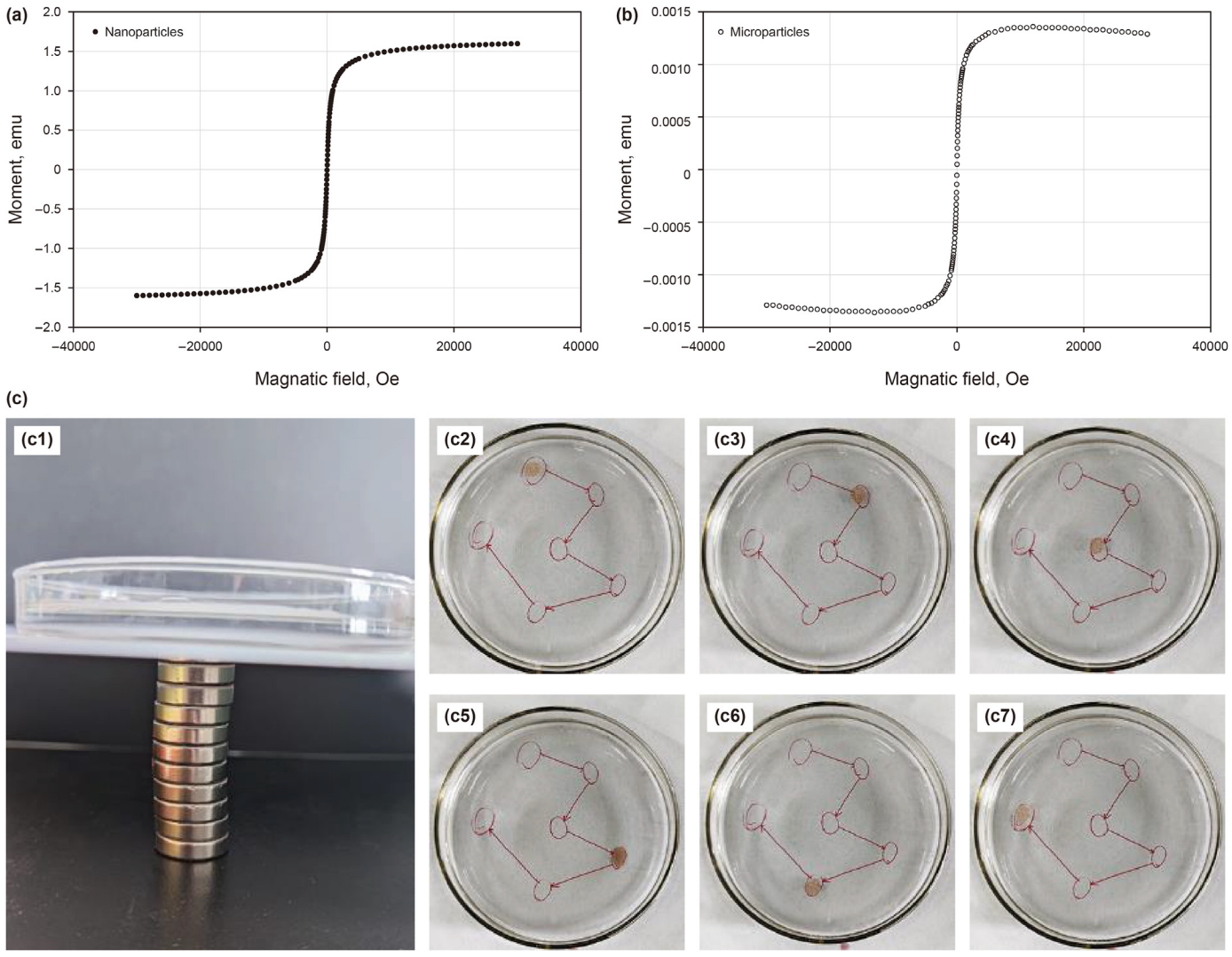

Fig. 4. Magnetic property of the core-shell microparticles. (**a**) The magnetic hysteresis curves of magnetic Fe_3O_4 particles. (**b**) Core-shell microparticles. (**c**) Collecting and moving the core-shell microparticles along a pre-set route with a magnet.

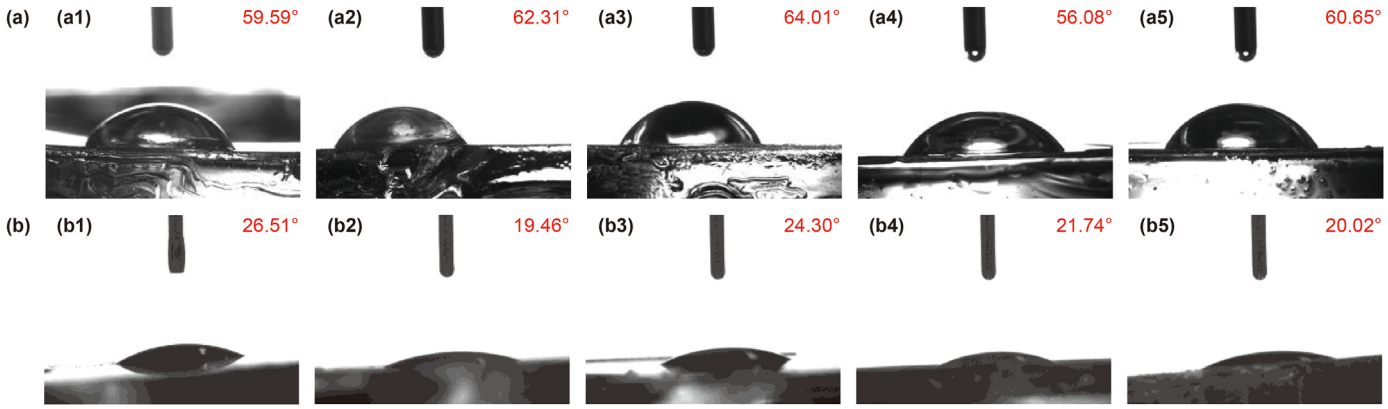

Fig. 5. The contact angles of DI water and diesel oil on PETPTA planes. (**a**) The contact angles of DI water and (**b**) diesel oil on PETPTA planes. The volume fraction of benzyl benzoate in the solution for PETPTA planes fabrication are 0% (**a1**, **b1**), 10% (**a2**, **b2**), 20% (**a3**, **b3**), 30% (**a4**, **b4**) and 40% (**a5**, **b5**), respectively.

3.5. Temperature-dependent equilibrium volume change of PNIPAM microgels in core-shell microparticles

PNIPAM microgels work as pistons in core-shell microparticles due to their excellent thermal-sensitive property, and temperature-dependent equilibrium volume change is a pivotal parameter for PNIPAM microgels. The microgel in the microparticle gradually shrinks as the temperature rises from 23 to 40 °C (Fig. 6a), and swells as the temperature drops from 40 to 23 °C (Fig. 6b). The equilibrium volume change of PNIPAM microgels when ambient temperature changes from 23 to 40 °C is shown in Fig. 6c, an obvious volume change of the PNIPAM microgels appeared at around 32 °C. In addition, when the ambient temperature was 40 °C, the minimum, maximum and average diameters were 68.48、148.43, and 98.35 μm respectively; the minimum, maximum, and average of reduced volume were 6.76×10^5, 41.12×10^5 and 26.12×10^5 μm^3 respectively; the minimum, maximum and average of volume change ratio were 8.71%, 87.24%, and 25.59% respectively. According to the previous research (Mao et al., 2014), the volume shrinkage and expansion rates of PNIPAM microgels and the temperature nodes at which significant volume changes match with PNIPAM microgels, confirming the simultaneous polymerization of NIPAM and ETPTA did not affect the thermal-sensitive property of the hydrogels. Therefore, the microparticles have a prominent thermal-sensitive property to provide sufficient cavities to adsorb oil.

3.6. Adsorption/regeneration test

3.6.1. Microscopic characterization of oil adsorption/regeneration process of core-shell microparticles

Fig. 7a and Movie S1 show that the adsorption process of diesel oil by core-shell microparticles is recorded by an optical microscope. When the ambient temperature was 40 °C, the PNIPAM cores of the core-shell microparticles shrunk quickly, and diesel oil dyed by Sudan III started to flow into the core-shell microparticles via the hole, the microparticles were filled with the diesel oil after 5 min (Fig. 7a). Subsequently, the microparticles adsorbing diesel oil were transferred to DI water, diesel oil was regenerated quickly and the PNIPAM cores of the microparticles swelled rapidly with shaking slightly at the ambient temperature of 23 °C (Fig. 7b and Movie S2).

In the adsorption process, the microparticles were added to oily

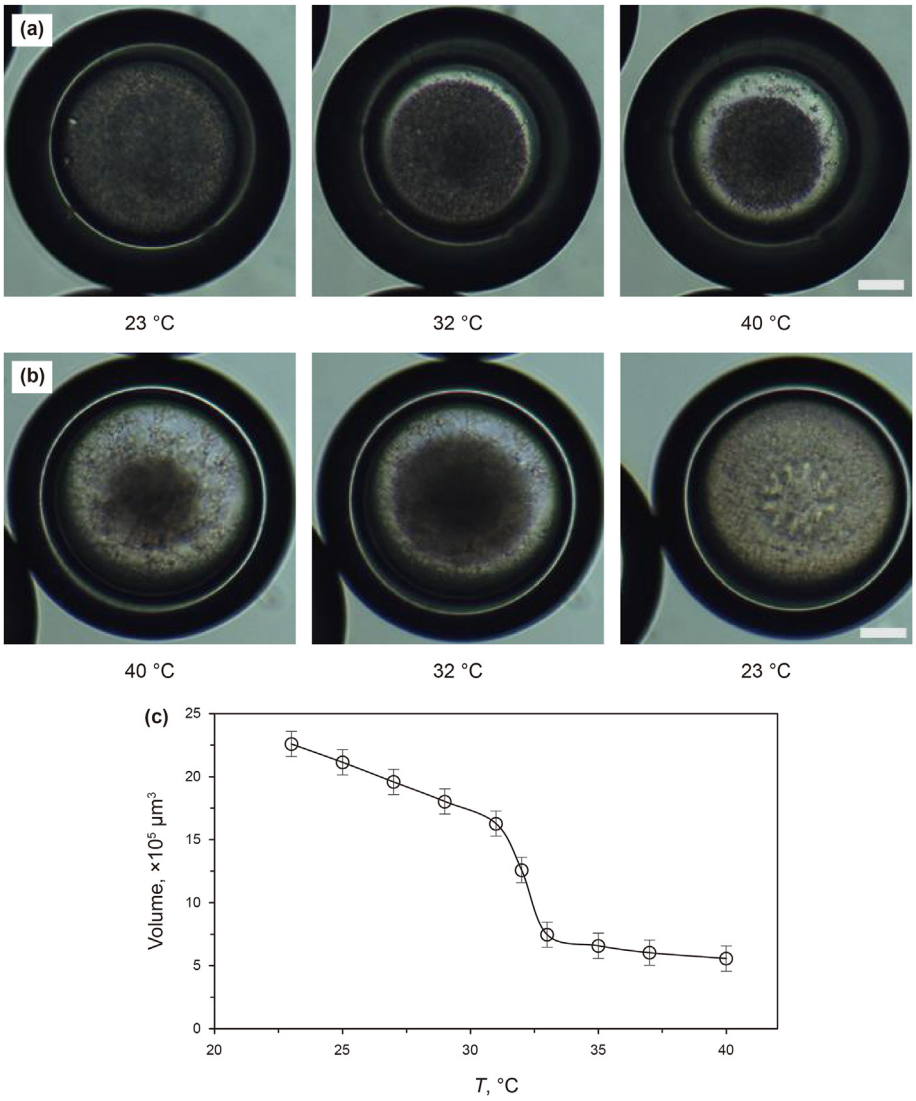

Fig. 6. Temperature-dependent equilibrium behaviors of the core-shell microparticles. Optical micrographs of core-shell microparticles in DI water at different temperatures (**a**, **b**) and the corresponding volume-change curve (**c**). Scale bar is 50 μm.

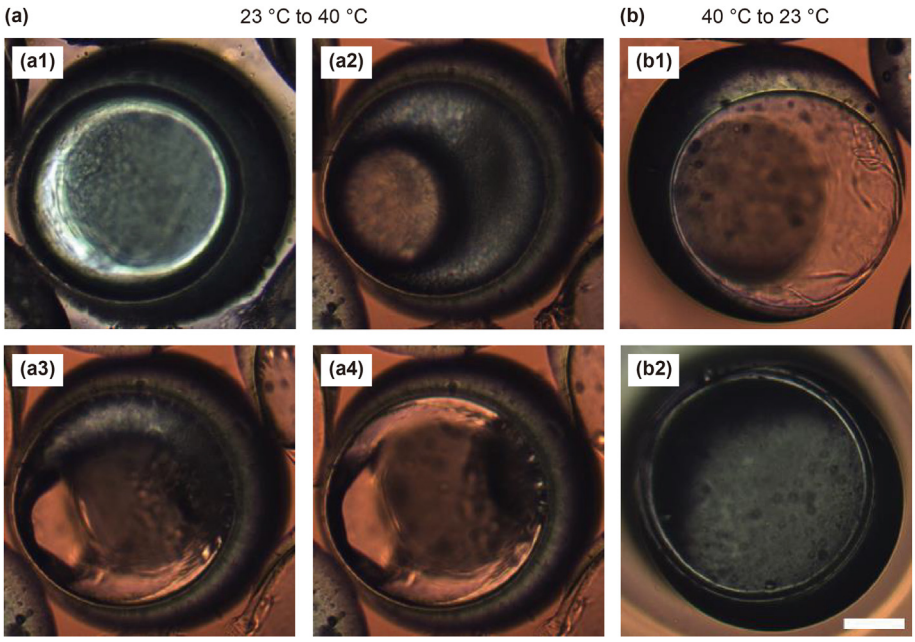

Fig. 7. Controlled adsorption/releasing diesel oil by core-shell microparticles. (**a**) Optical micrographs of core-shell microparticles absorbing the red-dyed diesel oil when the temperature is rose from 23 °C to 40 °C. (**b**) Optical micrographs of core-shell microparticles releasing the captured oil by volume expansion of inner PNIPAM core when the temperature is decreased from 40 °C to 23 °C. Scale bar is 50 μm.

wastewater, they quickly accumulate into clusters due to the microparticles each takes a highly lipophilic shell and thus the surface could adsorb the oil. When the temperature increased from 23 to 40 °C or more, the core hydrogel rapidly shrunk to release water. Due to the pressure difference between both sides of the interface, as shown in Fig. S3, the oil would be adsorbed into the microparticles. The pressure difference between the oil-water interface is formed due to the different interfacial tensions of the oil-water phases, and the interface is curved. So that the substance exchange between the core of the microparticles and the outside can be carried out through the pores, to achieve the adsorption of the oil by the microparticles.

In the regeneration process, the oil-adsorbed microparticles were transferred to a bottle with water, and the temperature was changed from 40 to 23 °C. According to the literature (Tanaka and Fillmore, 1979), the PNIPAM microgels swelled due to gel networks adsorbing water from surrounding when the temperature was below 32 °C, but the microgels of microparticles were surrounded by oil. Therefore, the swelling process of the hydrogels needed to be assisted by shaking, which made shrinking hydrogel in contact with the water, and the swelled hydrogels forced out the oil in the core for regeneration. The result indicates that the single hole of the microparticle plays a crucial role in the process of material exchange inside and outside of microparticles.

3.6.2. *Macroscopic characterization of oil adsorption/regeneration process of core-shell microparticles*

Fig. 8 shows the adsorption/regeneration process of diesel oil by core-shell microparticles in three ways. (1) The diesel oil dyed by Sudan III was smeared on the surface of the DI water in a petri dish (Fig. 8a1), then the petri dish was placed in the thermostat water bath; at the same time, the core-shell microparticles were scattered randomly on the surface, Fig. 8a2 shows that the microparticles accumulated quickly into clusters; subsequently, the diesel oil was adsorbed completely by the core-shell microparticles (Fig. 8a3); finally, the microparticles adsorbing diesel oil were collected by a magnet (Fig. 8a4). (2) The core-shell microparticles were placed in the pipe with DI water and immobilized by a magnet (Fig. 8b1); the homogeneous mixture of DI water and diesel oil dyed by Sudan III at 50 °C was poured into the pipe after being heated to 50 °C (Fig. 8b2); the microparticles change from light yellow to red (Fig. 8b3 and b4). (3) The core-shell microparticles were placed in a bottle with a homogeneous mixture of DI water and diesel oil dyed by Sudan III (Fig. 8c1); the microparticles changed from light yellow to red and the homogeneous mixture changed from muddy to transparent via a heating process in the thermostat water bath (Fig. 8c2); the microparticles faded and the solution became muddy again with shaking slightly at 23 °C (Fig. 8d1); the DI water and diesel oil in the solution were stratified for a while (Fig. 8d2). The above results illustrate that the core-shell microparticles have a significant adsorption performance for diesel oil in three scenarios. The core-shell microparticles are thousands of times smaller in volume compared to polyurethane sponges and aerogels (Le et al., 2020; Yu et al., 2020), which can be more flexibly applied in various scenarios.

3.6.3. *Quantitative analysis of oil adsorption/regeneration of microparticles*

Highly efficient and stable separation performance is of great importance for microparticles in long-term oily wastewater treatment. Notably, the thermal driving regeneration property is a crucial factor to keep the recycling of the microparticles and avoid secondary pollution. Therefore, cyclic experiments were carried out to analyze the adsorption capacity and the reusability of the microparticles in the adsorption/regeneration process. Fig. 9a shows that the cyclic adsorption capacity of core-shell microparticles generated from W/O/W emulsions with BB volume fractions of 0%, 10%, and 20% for diesel oil respectively, and the average adsorption quantity of microparticles reached 3.389, 3.282 and 3.099 g/g respectively. According to the description of section 3.2, the pore size of the microparticles could be precisely controlled by the different BB volume fractions in emulsions. The pore size distribution frequency of microparticles generated from emulsions with BB fractions of 0%, 10%, 20%, 30%, and 40% respectively, and their

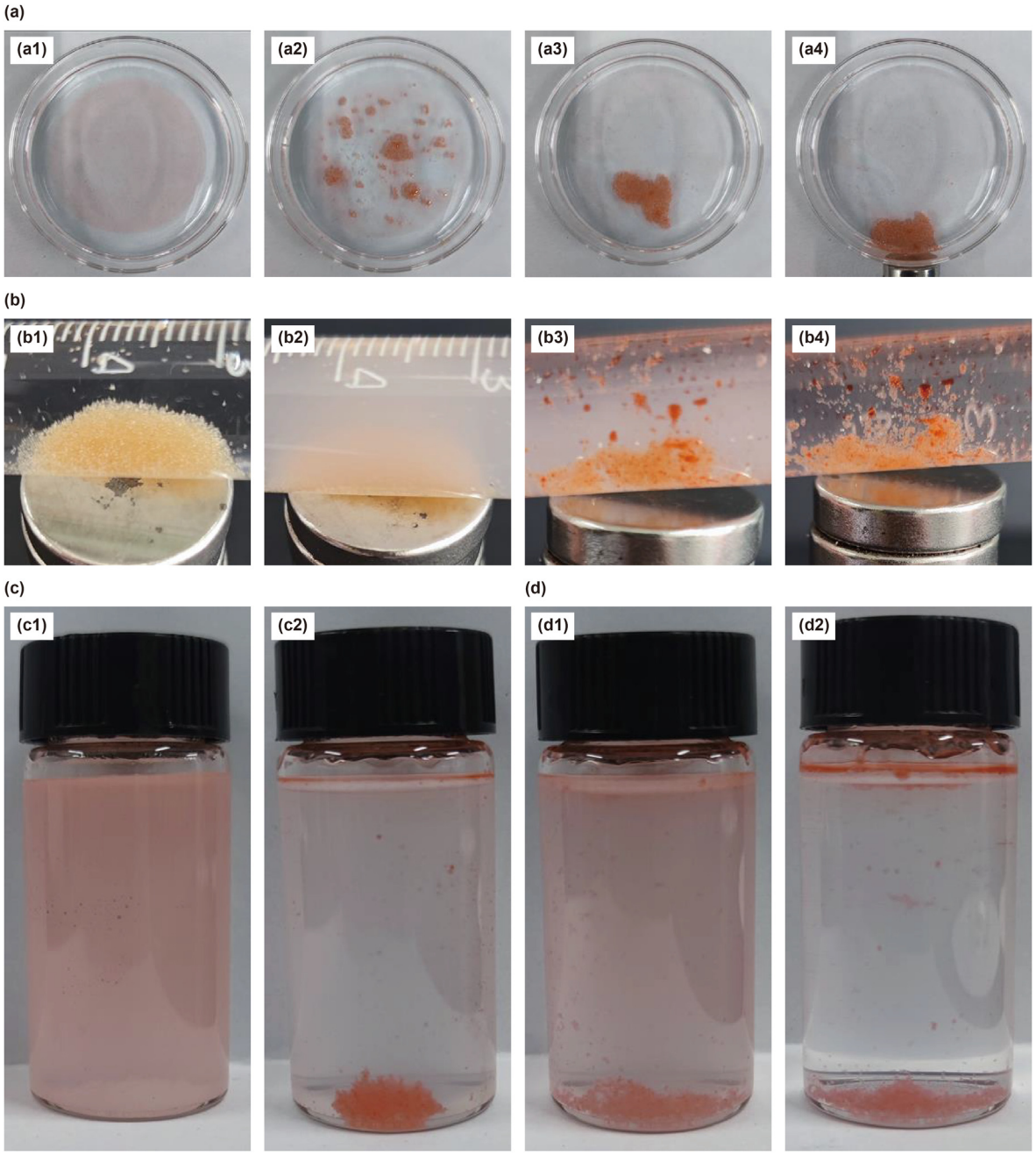

Fig. 8. Absorption of diesel oil by core-shell microparticles. (**a**) Adsorption of diesel oil floating on the water surface into core-shell microparticles in a petri dish. The diesel oil will float on the water surface due to the density difference (**a1**), and will be absorbed into the core-shell microparticles by controlling the temperature (**a2**). The core-shell microparticles with absorbed oil could be collected by a magnet (**a3**, **a4**). (**b**) The magnet fixed core-shell microparticles absorbing the emulsified diesel oil from flowing water in a pipe at 50 °C. (**c**) Adsorption and releasing dispersed diesel oil in a bottle. When the core-shell microparticles is placed into aqueous solution with emulsified diesel oil, the diesel oil will be absorbed into the core-shell microparticles by rising the temperature from 23 to 40 °C (**c1**, **c2**). The core-shell microparticles could release the absorbed and be regenerated by decreasing the temperature from 40 to 23 °C (**d1**, **d2**).

pore sizes were mainly distributed in 54 ± 2, 64 ± 2, 76 ± 2, 92 ± 2, and 98 ± 2 μm respectively (Fig. S1). Therefore, the increase of BB volume fraction in emulsions could cause adsorption capacity of the microparticles for diesel oil to decrease gradually and adsorption time of the microparticles for diesel oil to decrease from 80 min to 5 min (Fig. S4). The driving force and the resistance of oil adsorbed into the core-shell microparticles decreases simultaneously while the size of the PETPTA shells increases. The interfacial tension induced forces will drive the oil to be absorbed into the core-shell microparticles (Fig. S3). According to the Laplace Eq. (4), the pressure difference is affected by the interfacial tension and the surface radius at the interface.

$$\Delta p = \gamma\left(\frac{1}{R_1}+\frac{1}{R_2}\right) \tag{4}$$

Δp represents the pressure difference between both sides of the interface; γ represents the interfacial tension of the liquid film; R_1 and R_2 represent any two orthogonal radii of curvature of a point on the interface under the action of additional pressure Δp. When the

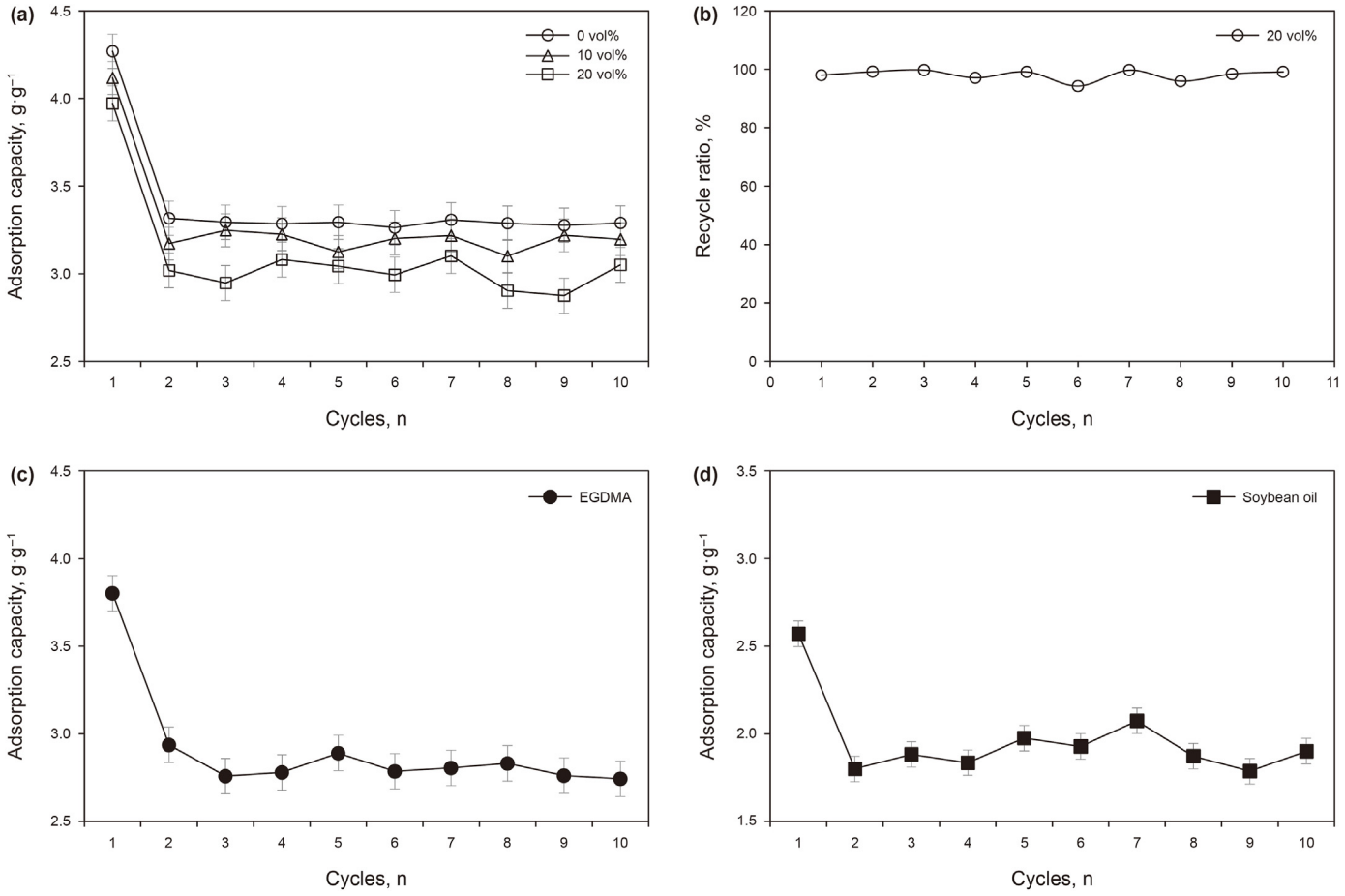

Fig. 9. Cyclic adsorption properties of the core-shell microparticles. (**a**) The adsorption ability of the core-shell microparticles to diesel oil are influenced by the benzyl benzoate content in the corresponding W/O/W emulsions templates. (**b**) The recovery ratio of the core-shell microparticles to diesel oil. (**c**) The adsorption ability of the core-shell microparticles to EGDMA and (**d**) soybean oil in the cycling of sorption/desorption experiment. The benzyl benzoate in the middle oil phase of W/O/W emulsions templates for core-shell microparticles are 20% (v/v) in (**b**), (**c**) and (**d**).

surface is spherical, $R_1 = R_2 = R$, which is proportional to the pore size on the shells. Therefore, the driving force for adsorption is $\Delta p_1 = \frac{2\gamma}{R'}$, in Fig. S3a, which is greater than $\Delta p_2 = \frac{2\gamma}{R''}$ in Fig. S3b. The smaller the pore size is, the larger the Δp is.

However, the rate of adsorption will be further affected by the flow resistance of the oil into the PETPTA shells, which varies with viscosity and flow rate of adsorbed oil. The low rate of oil adsorbed into the microparticles is hard to measure experimentally. All in all, the driving force and the resistance of the oil adsorbed into core-shell microparticles decrease simultaneously while the size of the pores increases, which makes the adsorption rate of oil into the core-shell microparticles hard to calculate theoretically. Therefore, we compared the adsorption rate of the core-shells microparticles with different pore sizes experimentally.

Moreover, after the first cycle, the adsorption capacity of the microparticles for diesel oil reduced significantly for the other nine cycles. The microparticles will quickly accumulate into clusters in the oily wastewater because of the lipophilic shells. We regenerate the microparticles by cooling and shaking. However, part of the oil on the outer surface of the microparticles is hard to remove in the regeneration process of 1st cycle, resulting in a significant decrease in adsorption capacity. After the 1st cycle, the content of adsorbed oil on the outer surface of the microparticles will change little. Therefore, there is no significant change in the adsorption capacity in the following cycles. The adsorption of oil on the outer surface has been further characterized, as shown in Fig. S5. The microparticles are dispersed in water at the initial time and display a slightly yellow color (Fig. S5a1–c1). The red-colored diesel oil is adsorbed into the core and on the outer surface of the microparticles after the absorption process. The microparticles will accumulate in clusters in water with a red color (Fig. S5a2–c2). After regeneration by temperature varying, the adsorbed oil in the cores will be forced out. However, some diesel oil on the surface of the microparticles can't be removed completely after the first cycle (Fig. S5a3–c3), which makes the adsorption capacity decline significantly. After the 1st cycle, the content of adsorbed oil on the outer surface of the microparticles will change little. Therefore, there is no significant change in the adsorption capacity in the following cycles. More importantly, the adsorbed oil in microparticles could be recycled by distillation while the microparticles have been regenerated with water.

The adsorption capacity rises along with the inner core sizes of the PETPTA shells. However, an oversized core can lead to an overly thin shell thickness, which will reduce the mechanical strength of the microparticles and lead to unexpected cracking of the PETPEA shells in use. Therefore, the core-shell microparticles generated from the oil phase containing 20 vol% BB in emulsions were used in the next adsorption experiments. Fig. 9b shows the recovery ratio of the microparticles for diesel oil, which is a ratio of the recovery capacity and adsorption capacity of the microparticles. It presents the microparticles that can be used to recycle oil from wastewater.

MOF material AM-rGA has a high adsorption capacity (over 45 g/g) and efficient adsorption rate (within 5 s) (Sun et al., 2020). The adsorption capacity of PTPGDA microspheres for diesel oil could reach 3.38 g/g in a few seconds (Yu et al., 2020). However, the adsorbents have been regenerated by vacuum drying and organic solvents, which will cause secondary pollution and the loss of oils. Although the core-shell microparticles do not exhibit an advantage in terms of adsorption volume and adsorption time, the thermal driving regeneration property of the microparticles can replace organic solvent regeneration to avoid secondary pollution. Besides, another benefit of the regeneration methods is that valuable oils can be recycled to improve economic efficiency. Fig. 9c and d shows the cyclic adsorption capacity of the microparticles generated from W/O/W emulsions with a BB volume fraction of 20% for soybean oil and EGDMA. And the average adsorption quantities of the microparticles for EGDMA and soybean oil reach 1.962 and 2.909 g/g respectively. Therefore, the core-shell microparticles have maintained stable and highly efficient adsorption performance for various oil.

4. Conclusions

In summary, we have engineered core-shell microparticles each with a single-holed magnetic PETPTA (poly (ethoxylated trimethylolpropane triacrylate)) shell and a thermal-sensitive PNIPAM (poly (*N*-Isopropylacrylamide)) core by using the microfluidic method, which could be used to remove oil from water and regenerated by a thermal stimulus. Monodispersed W/O/W emulsion templates from microfluidics are evolved to different structures by adjusting the interfacial tensions in emulsions. Core-shell microparticles with varied structures and hole sizes on shells are prepared by polymerization of the evolved W/O/W emulsions. The resulting microparticles could adsorb oil from water due to the pressure differential induced by the special holed structure on the shells and the thermal-sensitive cores. The oil adsorption performance of the microparticles is optimized by tailoring the size of the holes on outer PETPTA shells. The core-shell microparticles show stable adsorption capacity and high adsorption efficiency to several types of oil in the cyclic adsorption experiment. The core-shell microparticles could be regenerated by thermal stimulus, in which the PNIPAM cores will swell to force out the absorbed oil. The core-shell microparticles provide us a chance to recycle oil from water without secondary pollution. Therefore, the proposed core-shell microparticles show excellent oil adsorb and thermal driving regeneration performance, which would have application prospects in many fields, such as petroleum industry, pollution treatment.

Acknowledgments

This work was supported by the National Natural Science Foundation of China [grant numbers 21706219]

Appendix A. Supplementary data

Supplementary data to this article can be found online at https://doi.org/10.1016/j.petsci.2023.02.010.

References

Abbaspourrad, A., Carroll, N.J., Kim, S.H., Weitz, D.A., 2013. Surface functionalized hydrophobic porous particles toward water treatment application. Adv. Mater. 25 (23), 3215–3221. https://doi.org/10.1002/adma.201300656.

Adetunji, A.I., Olaniran, A.O., 2021. Treatment of industrial oily wastewater by advanced technologies: a review. Appl. Water Sci. 11 (6), 98. https://doi.org/10.1007/s13201-021-01430-4.

Beyer, J., Trannum, H.C., Bakke, T., Hodson, P.V., Collier, T.K., 2016. Environmental effects of the deepwater horizon oil spill: a review. Mar. Pollut. Bull. 110 (1), 28–51. https://doi.org/10.1016/j.marpolbul.2016.06.027.

Broje, V., Keller, A.A., 2007. Effect of operational parameters on the recovery rate of an oleophilic drum skimmer. J. Hazard Mater. 148 (1–2), 136–143. https://doi.org/10.1016/j.jhazmat.2007.02.017.

Chen, K.L., Zhou, S.X., Yang, S., Wu, L.M., 2015. Fabrication of all-water-based self-repairing superhydrophobic coatings based on UV-responsive microcapsules. Adv. Funct. Mater. 25 (7), 1035–1041. https://doi.org/10.1002/adfm.201403496.

de Medeiros, A.D.M., da Silva, J.C.G., de Amorim, J.D.P., Durval, I.J.B., Costa, A.F.D., Sarubbo, L.A., 2022. Oily wastewater treatment: methods, challenges, and trends. Processes 10 (4), 743. https://doi.org/10.3390/pr10040743.

Doan, H.N., Vo, P.P., et al., 2021. Environmentally friendly chitosan-modified polycaprolactone nanofiber/nanonet membrane for controllable oil/water separation. Acs Applied Polymer Materials 3 (8), 3891–3901. https://doi.org/10.1021/acsapm.1c00463.

Dutra, G.V.S., Araujo, O.A., Neto, W.S., Garg, V.K., Oliveira, A.C., Junior, A.F., 2017. Obtaining superhydrophopic magnetic nanoparticles applicable in the removal of oils on aqueous surface. Mater. Chem. Phys. 200, 204–216. https://doi.org/10.1016/j.matchemphys.2017.07.070.

El-Samak, A.A., Ponnamma, D., Hassan, M.K., Ammar, A., Adham, S., Al-Maadeed, M.A., Karim, A., 2020. Designing flexible and porous fibrous membranes for oil water separation-a review of recent developments. Polym. Rev. 60 (4), 671–716. https://doi.org/10.1080/15583724.2020.1714651.

Gu, J.J., Jiang, W., Wang, F.H., Chen, M.D., Mao, J.Y., Xie, T., 2014. Facile removal of oils from water surfaces through highly hydrophobic and magnetic polymer nanocomposites. Appl. Surf. Sci. 301, 492–499. https://doi.org/10.1016/j.apsusc.2014.02.112.

Guzowski, J., Korczyk, P.M., Jakiela, S., Garstecki, P., 2012. The structure and stability of multiple micro-droplets. Soft Matter 8 (27), 7269–7278. https://doi.org/10.1039/c2sm25838b.

Le, D.K., Ng, G.N., Koh, H.W., Zhang, X.W., Thai, Q.B., Phan-Thien, N., Duong, H.M., 2020. Methyltrimethoxysilane-coated recycled polyethylene terephthalate aerogels for oil spill cleaning applications. Mater. Chem. Phys. 239, 122064. https://doi.org/10.1016/j.matchemphys.2019.122064.

Li, X.B., Liu, J.T., Wang, Y.T., Xu, H.X., Cao, Y.J., Deng, X.W., 2015. Separation of oil from wastewater by coal adsorption-column flotation. Separ. Sci. Technol. 50 (4), 583–591. https://doi.org/10.1080/01496395.2014.956759.

Lin, B., Chen, J., Li, Z.T., He, F.A., Li, D.H., 2019. Superhydrophobic modification of polyurethane sponge for the oil-water separation. Surf. Coating. Technol. 359, 216–226. https://doi.org/10.1016/j.surfcoat.2018.12.054.

Liu, T.Q., Li, Z.J., Shi, G.M., Zhao, Q., Chen, X., Chen, X.L., Li, Y.L., 2019. Facile preparation of Fe_3O_4@C/Cu core-shell sub-micron materials for oil removal from water surface. Appl. Surf. Sci. 466, 483–489. https://doi.org/10.1016/j.apsusc.2018.10.026.

Lu, T., Zhang, S., Qi, D.M., Zhang, D., Vance, G.F., Zhao, H.T., 2017. Synthesis of pH-sensitive and recyclable magnetic nanoparticles for efficient separation of emulsified oil from aqueous environments. Appl. Surf. Sci. 396, 1604–1612. https://doi.org/10.1016/j.apsusc.2016.11.223.

Lu, T., Qi, D.M., Zhang, D., Fu, K.J., Li, Y., Zhao, H.T., 2020. Fabrication of recyclable multi-responsive magnetic nanoparticles for emulsified oil-water separation. J. Clean. Prod. 255, 120293. https://doi.org/10.1016/j.jclepro.2020.120293.

Lv, X.S., Tian, D.H., Peng, Y.Y., Li, J.X., Jiang, G.M., 2019. Superhydrophobic magnetic reduced graphene oxide-decorated foam for efficient and repeatable oil-water separation. Appl. Surf. Sci. 466, 937–945. https://doi.org/10.1016/j.apsusc.2018.10.110.

Ma, J.Y., Xia, W., Zhang, R., Ding, L., Kong, Y.L., Zhang, H.W., Fu, K., 2021. Flocculation of emulsified oily wastewater by using functional grafting modified chitosan: the effect of cationic and hydrophobic structure. J. Hazard Mater. 403, 123690. https://doi.org/10.1016/j.jhazmat.2020.123690.

Mao, J.Y., Jiang, W., Gu, J.J., Zhou, S., Lu, Y., Xie, T., 2014. Synthesis of P(St-DVB)/Fe_3O_4 microspheres and application for oil removal in aqueous environment. Appl. Surf. Sci. 317, 787–793. https://doi.org/10.1016/j.apsusc.2014.08.191.

Mi, T.W., Cai, Y.X., Wang, Q., Habibul, N., Ma, X.L., Su, Z., Wu, W., 2020. Synthesis of Fe_3O_4 nanocomposites for efficient separation of ultra-small oil droplets from hexadecane-water emulsions. RSC Adv. 10 (17), 10309–10314. https://doi.org/10.1039/d0ra01044h.

Mou, C.L., He, X.H., et al., 2012. Change in size and structure of monodisperse poly(N-isopropylacrylamide) microcapsules in response to varying temperature and ethyl gallate concentration. Chem. Eng. J. 210, 212–219. https://doi.org/10.1016/j.cej.2012.08.095.

Mou, C.L., Ju, X.J., et al., 2014. Monodisperse and fast-responsive Poly(N-isopropylacrylamide) microgels with open-celled porous structure. Langmuir 30 (5), 1455–1464. https://doi.org/10.1021/la4046379.

Mou, C.L., Wang, W., et al., 2018. Trojan-Horse-Like stimuli-responsive microcapsules. Adv. Sci. 5 (6), 1700960. https://doi.org/10.1002/advs.201700960.

Omarova, M., Swientoniewski, L.T., et al., 2019. Biofilm formation by hydrocarbon-degrading marine bacteria and its effects on oil dispersion. ACS Sustain. Chem. Eng. 7 (17), 14490–14499. https://doi.org/10.1021/acssuschemeng.9b01923.

Pan, Y.N., Wang, J.J., Sun, C.Y., Liu, X.Y., Zhang, H.X., 2016. Fabrication of highly hydrophobic organic-inorganic hybrid magnetic polysulfone microcapsules: a lab-scale feasibility study for removal of oil and organic dyes from environmental aqueous samples. J. Hazard Mater. 309, 65–76. https://doi.org/10.1016/j.jhazmat.2016.02.004.

Peng, Z.L., Xiong, C.M., Wang, W., Tan, F.T., Wang, X.Y., Qiao, X.L., Wong, P.K., 2018.

Hydrophobic modification of nanoscale zero-valent iron with excellent stability and floatability for efficient removal of floating oil on water. Chemosphere 201, 110–118. https://doi.org/10.1016/j.chemosphere.2018.02.149.
Poulin, P., Bibette, J., 1998. Adhesion of water droplets in organic solvent. Langmuir 14 (22), 6341–6343. https://doi.org/10.1021/la9801413.
Qiu, J., 2010. China faces up to groundwater crisis. Nature 466 (7304), 308. https://doi.org/10.1038/466308a.
Rojas-Alva, U., Andersen, B.S., Jomaas, G., 2019. Chemical herding of weathered crude oils for in-situ burning. J. Environ. Manag. 250, 109470. https://doi.org/10.1016/j.jenvman.2019.109470.
Shao, S.M., Li, Y., Lu, T., Qi, D.M., Zhang, D., Zhao, H.T., 2019. Removal of emulsified oil from aqueous environment by using polyvinylpyrrolidone-coated magnetic nanoparticles. Water 11 (10), 1993. https://doi.org/10.3390/w11101993.
Shi, Y., Li, S.W., Zhang, H.Q., Peng, S.T., Chen, H.B., 2017. Experimental studies on performances of flexible floating oil booms in coupled wave-current flow. Appl. Ocean Res. 69, 38–52. https://doi.org/10.1016/j.apor.2017.10.001.
Soares, M.D., Teixeira, C.E.P., et al., 2020. Oil spill in south atlantic (Brazil): environmental and governmental disaster. Mar. Pol. 115, 103879. https://doi.org/10.1016/j.marpol.2020.103879.
Sun, T.C., Hao, S.E., Fan, R.Q., Qin, M.Y., Chen, W., Wang, P., Yang, Y.L., 2020. Hydrophobicity-adjustable MOF constructs superhydrophobic MOF-rGO aerogel for efficient oil-water separation. ACS Appl. Mater. Interfaces 12 (50), 56435–56444. https://doi.org/10.1021/acsami.0c16294.
Sun, T.L., Qing, G.Y., 2011. Biomimetic smart interface materials for biological applications. Adv. Mater. 23 (12), H57–H77. https://doi.org/10.1002/adma.201004326.
Tanaka, T., Fillmore, D.J., 1979. Kinetics of swelling of gels. J. Chem. Phys. 70 (3), 1214–1218. https://doi.org/10.1063/1.437602.
Tao, S.Y., Ding, Y.Z., Jiang, L., Li, G.T., 2017. Preparation of magnetic hierarchically porous microspheres with temperature-controlled wettability for removal of oils. J. Colloid Interface Sci. 492, 73–80. https://doi.org/10.1016/j.jcis.2016.12.069.
Theurer, J., Ajagbe, O., Osorio, J., Elgaddafi, R., Ahmed, R., Walters, K., Abbott, B., 2020. Removal of residual oil from produced water using magnetic nanoparticles. SPE J. 25 (5), 2482–2495. https://doi.org/10.2118/199466-PA.
Wang, Q., Yang, Z.M., 2016. Industrial water pollution, water environment treatment, and health risks in China. Environ. Pollut. 218, 358–365. https://doi.org/10.1016/j.envpol.2016.07.011.
Wang, W., Zhang, M.J., et al., 2013. Hole-Shell microparticles from controllably evolved double emulsions. Angew. Chem. Int. Ed. 52 (31), 8084–8087. https://doi.org/10.1002/anie.201301590.
Whitehead, A., Dubansky, B., et al., 2012. Genomic and physiological footprint of the deepwater horizon oil spill on resident marsh fishes. Proc. Natl. Acad. Sci. U.S.A. 109 (50), 20298–20302. https://doi.org/10.1073/pnas.1109545108.
Wu, D.L., Honciuc, A., 2018. Design of Janus nanoparticles with pH-triggered switchable amphiphilicity for interfacial applications. ACS Appl. Nano Mater. 1 (1), 471–482. https://doi.org/10.1021/acsanm.7b00356.
Wu, F., Pickett, K., Panchal, A., Liu, M.X., Lvov, Y., 2019. Superhydrophobic polyurethane foam coated with polysiloxane-modified clay nanotubes for efficient and recyclable oil absorption. ACS Appl. Mater. Interfaces 11 (28), 25445–25456. https://doi.org/10.1021/acsami.9b08023.
Yan, S.W., Li, Y., et al., 2020. Environmentally safe and porous MS@TiO2@PPy monoliths with superior visible-light photocatalytic properties for rapid oil-water separation and water purification. ACS Sustain. Chem. Eng. 8 (13), 5347–5359. https://doi.org/10.1021/acssuschemeng.0c00360.
Yan, T., Zhang, T.H., Zhao, G.Q., Zhang, C.Y., Li, C.F., Jiao, F.P., 2019. Magnetic textile with pH-responsive wettability for controllable oil/water separation. Colloids Surf. A Physicochem. Eng. Asp. 575, 155–165. https://doi.org/10.1016/j.colsurfa.2019.04.083.
Yang, M.P., Liu, W.Q., Jiang, C., Xie, Y.K., Shi, H.Y., Zhang, F.Y., Wang, Z.F., 2019. Facile construction of robust superhydrophobic cotton textiles for effective UV protection, self-cleaning and oil-water separation. Colloids Surf. A Physicochem. Eng. Asp. 570, 172–181. https://doi.org/10.1016/j.colsurfa.2019.03.024.
Yu, L., Han, M., He, F., 2017. A review of treating oily wastewater. Arab. J. Chem. 10, S1913–S1922. https://doi.org/10.1016/j.arabjc.2013.07.020.
Yu, Y.L., Zhou, Z.H., Yu, W.T., Song, Y.Z., Xie, M.Q., 2020. Preparation of magnetic porous microspheres and their ability to remove oils. Macromol. Mater. Eng. 305 (1), 12. https://doi.org/10.1002/mame.201900452.
Zeinstra-Helfrich, M., Koops, W., Murk, A.J., 2017. Predicting the consequence of natural and chemical dispersion for oil slick size over time. J.Geophys. Res.Ocean 122 (9), 7312–7324. https://doi.org/10.1002/2017jc012789.